HHS Public Access

Author manuscript

Eur J Radiol. Author manuscript; available in PMC 2017 January 01.

Published in final edited form as:

Eur J Radiol. 2016 January ; 85(1): 136–142. doi:10.1016/j.ejrad.2015.11.003.

Crossed cerebellar diaschisis after stroke identified noninvasively with cerebral blood flow-weighted arterial spin labeling MRI

Megan K. Strother, MD[a], **Cari Buckingham, MD**[a], **Carlos C. Faraco, PhD**[a], **Daniel Arteaga, BS**[a], **Pengcheng Lu, MS**[b], **Yaomin Xu, PhD**[b], and **Manus J. Donahue, PhD**[a,*]

[a]Department of Radiology and Radiological Sciences, Vanderbilt Medical Center, Nashville, TN, USA

[b]Center for Quantitative Sciences, Vanderbilt Medical Center, Nashville, TN, USA

Abstract

Background and Purpose—Crossed cerebellar diaschisis (CCD) is most commonly investigated using hemodynamic PET and SPECT imaging. However, noninvasive MRI offers advantages of improved spatial resolution, allowing hemodynamic changes to be compared directly with structural findings and without concerns related to ionizing radiation exposure. The aim of this study was to evaluate relationships between CCD identified from cerebral blood flow (CBF)-weighted arterial spin labeling (ASL) MRI with cerebrovascular reactivity (CVR)-weighted blood oxygenation level dependent (BOLD) MRI, Wallerian degeneration, clinical motor impairment, and corticospinal tract involvement.

Methods—Subjects (n=74) enrolled in an ongoing observational stroke trial underwent CBF-weighted ASL and hypercapnic CVR-weighted BOLD MRI. Hemispheric asymmetry indices for basal cerebellar CBF, cerebellar CVR, and cerebral peduncular area were compared between subjects with unilateral supratentorial infarcts (n=18) and control subjects without infarcts (n=16). CCD required (1) supratentorial infarct and (2) asymmetric cerebellar CBF (>95% confidence interval relative to controls).

Results—In CCD subjects (n=9), CVR (p=0.04) and cerebral peduncular area ($p < 0.01$) were significantly asymmetric compared to controls. Compared to infarct subjects not meeting CCD criteria (n=9), CCD subjects had no difference in corticospinal tract location for infarct (p=1.0) or motor impairment (p=0.08).

*Corresponding author: Manus J. Donahue, PhD, Vanderbilt University Institute of Imaging Science, Rm. AAA-3115, 1161 21st Ave South, Nashville, TN, 37232, mj.donahue@vanderbilt.edu, 615.322.8350.

All work was carried out at the Vanderbilt Medical Center, Nashville, TN, USA

Conflicts of interests

No authors have any conflicts of interest to declare.

Conclusions—CCD correlated with cerebellar CVR asymmetry and Wallerian degeneration. These findings suggest that noninvasive MRI may be a useful alternative to PET or SPECT to study structural correlates and clinical consequences of CCD following supratentorial stroke.

Keywords

crossed cerebellar diaschisis; BOLD; fMRI; cerebrovascular reactivity; CBF; Wallerian degeneration

Introduction

Crossed cerebellar diaschisis (CCD) refers to a depression of CBF and metabolism affecting the cerebellar hemisphere contralateral to supratentorial lesions. CCD manifests as decreased cerebellar CBF and CBV, which is thought to be secondary to arterial vasoconstriction but with retained cerebrovascular reactivity (CVR) capacity [1; 2]. CCD has been predominantly studied through hemodynamic PET [3] and SPECT [4] imaging. While these imaging modalities have greatly improved our understanding of CCD, the radioactive tracers required limit their longitudinal monitoring potential, a characteristic that is necessary to understand the temporal progression and pathophysiology of CCD. Further, PET and SPECT lack the spatial resolution achieved with MRI, which is necessary to characterize structural findings that precipitate or result from CCD. Perfusion MRI utilizing exogenous contrast agents has had mixed results to date, is contraindicated in some patients, and in cases of ischemia remains largely qualitative in nature owing to difficulties in accurately quantifying regional arterial input functions [5]. Alternatively, noninvasive MRI methods for characterizing CCD would have few patient restrictions and thus are of particular interest for more readily evaluating novel stroke rehabilitation techniques [6] and functional outcomes [7; 8].

Yamada, et al. first characterized CCD with hemodynamic MRI utilizing DSC-MRI [7]. While this remains the most frequently reported MRI metric for CCD, some studies report DSC-MRI lacks sensitivity compared to PET [9]. When evaluating the body of work on CCD across all imaging modalities, two important limitations should be considered. First, posterior vascular stenosis has not always been considered [4; 7; 10]. Therefore, flow changes due to vertebral artery stenosis could impact the CCD cohort. Second, as most CCD studies have focused on hemodynamic findings identified with PET and SPECT, hemodynamic sequelae of CCD have been studied more thoroughly than the structural changes which cause or are associated with it, which are less well understood [1; 10; 11].

In a case study, noninvasive arterial spin labeling (ASL) MRI identified asymmetric CBF consistent with CCD [12]. Alternatively, CVR-weighting can readily be obtained using the well-established blood oxygenation level-dependent (BOLD) MRI approach in conjunction with a hypercapnic gas stimulus. To our knowledge, only one prior report used a noninvasive gas challenge with fMRI to study CCD, reporting cerebellar asymmetry with reduced CBV and CBF in acute MCA stroke subjects following a hyperoxic respiratory challenge [13].

The aims of the present study were to understand to what extent CCD correlated with (1) cerebellar CVR asymmetry from hypercapnic BOLD MRI (2) motor impairment (3) infarct location involving the corticospinal tract and (4) Wallerian degeneration. Our working hypothesis for using BOLD MRI in CCD is that reduced baseline CBF contralateral to the hemisphere with supratentorial infarcts will translate to a smaller vasoreactive response. In addition, we hypothesize CVR should be asymmetric between cerebellar hemispheres in a manner that reflects baseline hemodynamic tone in the face of preserved CVR capacity.

Materials and Methods

The goal of this work was to stratify patients with supratentorial infarcts into groups with vs. without cerebellar hemispheric asymmetry in CBF. For these two groups, we evaluated mean differences in (1) cerebellar CVR asymmetry (2) motor impairment (3) infarct location involving the corticospinal tract and (4) Wallerian degeneration. A control group without infarct was also included for comparison. Below we outline the details for this set of experiments.

Ethical considerations

The local Institutional Review Board approved this study and work was carried out in accordance with The Code of Ethics of the World Medical Association (Declaration of Helsinki). Subjects (n=74) were enrolled between January 2010 and June 2014 as part of the Assessment of Multimodal MRI in Patients at Risk for stroke with Intracranial Stenosis trial and provided informed, written consent.

MRI acquisition

All participants were scanned on the same scanner. All subjects underwent MRI at 3.0 Tesla with ASL, hypercapnic BOLD, and structural imaging; data were acquired with body coil radiofrequency transmission and a 16-channel multi-array SENSitivity Encoding (SENSE) head coil for reception.

For baseline CBF assessment, a pseudocontinuous ASL (pCASL) sequence was used with a 1.6s labeling pulse train consisting of Hanning-windowed 0.7 ms pulses, followed by a post-labeling delay of 1.525s (TR=4s; TE=13 ms; spatial resolution=3×3×7 mm^3). A separate equilibrium magnetization image was acquired with identical geometry but spin labeling preparation removed for M_0 calculation.

For CVR assessment, BOLD hypercapnic-hyperoxic (carbogen; 5% CO_2, 95% O_2) CVR-weighted scans were performed using a standard T_2*-weighted echo-planar imaging sequence (TR/TE=2000/35ms; spatial resolution = 3.5mm isotropic) in a block-design paradigm. The stimulus paradigm consisted of two blocks of 3 min hypercapnic hyperoxic administration interleaved with medical air (~21% O_2/~79% N_2/ <1% trace elements), all delivered at 12 L/min through a customized facemask setup. Physiological monitoring was achieved using an In Vivo Research Inc. device and Millennia Vital Systems Monitoring System (3155 MVS). Monitored parameters included heart rate, blood pressure, arterial oxygen saturation fraction (Y_a), and $EtCO_2$ (Salter Labs; Ref: 4000F).

For structural imaging, whole-brain T_1-weighted MPRAGE images with TR/TE=8.9/4.6ms, flip angle=8°, spatial resolution=1 mm isotropic; 2D turbo-inversion-recovery T2-FLAIR with TR/TE=11000/120, flip angle=90°, spatial resolution=0.9×1.0×5mm; and 3D T_1-weighted gradient echo time-of-flight angiography with TR/TE=13.9/1.9ms, flip angle=20°, spatial resolution=0.8×0.8×1.0mm were acquired.

MRI analysis

For basal CBF, ASL data were processed by an imaging physicist blinded to the structural analysis, surround-subtracted [14] and normalized by M_0 to generate CBF-weighted maps. CBF was quantified via application of the solution of the flow-modified Bloch equation [15]. To allow for comparison between subjects, all images were co-registered to a standard 4 mm T_1-weighted Montreal Neurological Institute atlas. Mean CBF for each cerebellar hemisphere was calculated within the Harvard-Oxford cerebellar atlas (region-of-interest shown in Results). Note that regions-of-interest were defined from standard cerebellar atlases for CBF analysis and the same regions were used in all subjects.

For CVR analysis, the same imaging physicist, blinded to structural imaging findings, analyzed the BOLD data, which were corrected for motion and baseline drift using standard affine correction algorithms. CVR was calculated as the z-statistic of the BOLD time course, which is defined as the magnitude of the signal change with hypercapnia normalized by the standard deviation of the baseline signal [16].

Infarct was determined by a board-certified neuroradiologist with criteria being lesion on FLAIR greater than 3 mm with confirming T_1 encephalopathy. For some patients, the image shown is only one lesion in a string of infarcts. The single punctate T_2 change may not meet 3 mm criteria alone but were included as infarct if in the setting of a string of T_2 changes in deep or subcortical white matter which are characteristic of watershed infarcts. The watershed pattern of infarcts was common in patients with Moyamoya disease. This pattern is distinct from periventricular white matter changes, which may not represent lacunar infarcts.

For Wallerian degeneration analysis, the area of the cerebral peduncles was measured from the T_1-weighted images separately by two neuroradiologists, blinded to clinical history and supratentorial findings, and CBF and CVR analysis outlined above. Peduncular area was manually drawn on the T_1-weighted axial images using the method of Mark, et al [17]. Using Medical Image Processing, Analysis & Visualization v7.0.1, a region-of-interest was drawn on the axial image with maximum peduncular width using a straight line to connect the oculomotor nerve sulcus in the prepontine cistern to the lateral sulcus of the midbrain, then filling in the peduncle and calculating the cross-sectional area (Figure 1).

Vertebrobasilar stenosis was classified by a neuroradiologist from angiography performed within 30 days of BOLD imaging (DSA, CTA, or MRA). Stenosis degree was classified as the ratio of the width of the stenosed lumen (measured in the plane with the most severe stenosis) to the width of the normal distal vessel.

Motor impairment determination

Clinical motor function was assessed retrospectively by a neurologist blinded to MRI findings using electronic medical records to determine motor function surrounding the time of the BOLD scan. Motor impairment related to the hemisphere with infarct was graded as: (1) normal motor function, (2) mild motor impairment (3) moderate motor impairment and (4) severe motor impairment. Similar to the modified Rankin scale [18], motor function was assessed as follows: mild motor impairment was slight difficulty, such as clumsiness or slowed motor movements. Moderate impairment was more significant motor difficulty requiring some help with activities of daily living or an assistive device such as a brace or a cane. Severe motor impairment was inability use the affected upper extremity or inability to walk if lower extremity was affected by the infarct.

Patient stratification

Subjects were stratified into three groups: (1) control, (2) non-CCD infarct group, and (3) CCD infarct. Criteria for group stratification are shown in Table 1 and outlined below.

First, control subjects with no infarcts (Table 2) were used to establish a range of expected asymmetry for CBF. A CBF asymmetry index (AI) was calculated for each control and infarct subject according to:

$$AI_{CBF} = \frac{Ipsilateral_{CBF} - Contralateral_{CBF}}{Ipsilateral_{CBF}}. \quad [1]$$

AIs were also calculated for mean peduncular area (e.g., Wallerian degeneration) and CVR in all subjects, however were not used as inclusion criteria:

$$AI_{WD} = \frac{Peduncle\ area\ ipsilateral - Penduncle\ area\ contralateral}{Peduncle\ area\ contralateral}, \quad [2]$$

and

$$AI_{CVR} = \frac{Ipsilateral_{CVR} - Contralateral_{CVR}}{Ipsilateral_{CVR}}. \quad [3]$$

A significant CBF asymmetry index (AI) for subjects with infarcts was defined as >95% confidence interval (CI) in control subjects [1; 2; 4]. Mean AI_{WD} and AI_{CVR} were calculated as well but not used as inclusion criteria as is convention.

Statistical analysis and hypothesis testing

Descriptive data were analyzed using either a Wilcoxon rank-sum test for continuous variables or χ^2 test or the Fisher exact test as appropriate for categorical variables. Comparison of AI variables between subjects with infarcts and controls was performed using the Wilcoxon rank-sum test. Correlations between raters on AI were determined with the Spearman correlation coefficient. Trend analysis was performed using the Jonchkheere-

Terpstra test. R software version 3.1.1 (http://www.R-project.org) was used for all analyses. Statistical significance was assessed at the two-sided $p<0.05$ level for all analyses.

Results

Control population

Of 74 subjects, 16 (10 females, 6 males; age=55.3+/−13.0 yrs) had no infarcts and met inclusion criteria for controls; AI for these controls are summarized in Table 2.

Infarct subjects

Subjects with supratentorial infarcts (48 of 74) were evaluated for the study, 20 of whom met the inclusion criteria. Two of these were excluded due to poor cerebellar coverage on hemodynamic imaging. The ages of the subjects evaluated (11 females, 7 males; age 47.8±16.1 yrs) did not differ significantly from the ages of the controls (p=0.09). Table 3 contains demographic information for these subjects.

Mean values for motor scores, and asymmetry indices in CCD subjects and subjects with infarcts who did not meet criteria for CCD (e.g., non-CCD subjects) are shown in Table 4. In subjects meeting criteria for CCD (n=9), CVR asymmetry index (p = 0.04) and cerebral peduncle area (e.g., Wallerian degeneration; $p < 0.01$) were significantly reduced compared to control subjects. Although AIWD did not meet statistical significance between CCD and non-CCD subjects (p = 0.05), it did meet statistical significance with trend analysis between CCD, non-CCD and control subjects ($p < 0.001$), as shown in Figure 2. All subjects with significant AI_{CVR} also met AI_{CBF} criteria for CCD, with significant AI_{CVR} in 7 of 9 CCD subjects. Compared to infarct subjects not meeting CCD criteria, CCD subjects had no significant difference in corticospinal tract location for infarct (p = 1.0) or for motor impairment (p = 0.08). There were no statistically significant differences in hemodynamic AI between non-CCD subjects and controls (AI_{WD} p = 0.14, AI_{CBF} p = 0.13, AI_{CVR} p = 0.45).

Representative images showing Wallerian degeneration, infarcts, and BOLD CVR for subjects with CCD are shown in Figure 3 and representative timecourse data for a CCD patient is shown in Figure 4.

Discussion

The major finding from this study was that subjects meeting imaging criteria for CCD (defined by reduced baseline cerebellar CBF contralateral to supratentorial infarct) showed significantly reduced cerebellar CVR compared to control subjects. Additionally, Wallerian degeneration correlated significantly with CCD, but infarct location in the CST and motor impairment did not. Findings suggest BOLD and Wallerian degeneration may provide noninvasive surrogates for CCD, correlating more closely with CCD than corticospinal tract involvement or motor impairment in chronic stroke subjects.

To our knowledge, this study is the first to characterize CCD using CVR-weighted hypercapnic BOLD fMRI. One prior study utilizing a gas challenge was a feasibility study,

in which significant asymmetric CBV and percentage signal changes were found after administering hyperoxic gas (100% O_2 in a block paradigm interleaved with normoxic room air) to a small number of acute MCA stroke subjects with large volume strokes [13]. Conclusions from a purely hyperoxic challenge do not translate to this study due to the vasoconstrictive or only moderately vasoactive properties of hyperoxia for short durations, which may induce delayed arterial arrival times, rather than reduced perfusion increases [13]. In contrast, a representative BOLD time course (Figure 4) is reduced rather than delayed compared to the contralateral cerebellar hemisphere.

Recently, MRI findings of Wallerian degeneration have been shown to be a valid biomarker for corticospinal tract degeneration likely resulting from axonal disintegration and myelin collapse following corticopontocerebellar tract degeneration [19]. Diffusion changes along this tract in acute stroke, which may represent early Wallerian degeneration, have been shown to predict motor outcome [20]. Although CCD has been shown to correlate with reduced fractional anisotropy along the corticospinal tract, results from one prior study correlating CCD from PET with fMRI were consistent with our results, finding not all subjects with CCD following chronic strokes have Wallerian degeneration [21]. While CCD has most commonly been associated with infarcts in areas involving the corticospinal tract, relationships between CCD and non-motor regions such as the thalamus [22], temporal association cortex and limbic system [23] have also been demonstrated [22]. In a study examining CCD with SPECT, *Komaba Y, et al.* [24] identified only the postcentral and supramarginal gyrus as independent determinants of CCD after controlling for confounding effects. Although CCD is a common manifestation after hemiparetic stroke [25], it has been documented in the absence of motor deficits [4; 26].

The correlation of impaired CVR with reduced CBF in our CCD subjects is consistent with prior studies reporting decreased CBF, CBV, and $CMRO_2$ in CCD subjects following CO_2 challenge with SPECT [3]. The BOLD signal represents a composite effect which can reflect CBF, CBV and $CMRO_2$. Additionally, CBF and $CMRO_2$ are uncoupled in CCD subjects, with larger decreases in CBF compared to $CMRO_2$ [1; 2]. Therefore, uncoupling of $CMRO_2$ with CBF/CBV following deafferentation could result in less of a reduction in $CMRO_2$ with hypercapnia in the affected hemisphere [11]. CBV, but not $CMRO_2$, has been shown to correlate with the percent change of CBF during acetazolamide administration in CCD subjects [11]. Preservation of cerebellar vasoreactivity with diminished CBF reflects reduced metabolic requirements [3; 10].

In this study we utilized a hypercapnic hyperoxic gas stimulus, which was required by our institution as a safety measure in subjects with cerebrovascular disease to ensure that the fraction of inspired oxygen would not reduce. Other hospitals may require similar safety precautions. It is important to note that BOLD effects will vary uniquely between this stimulus and hypercapnic normoxic stimuli [27], but both hypercapnic stimuli cause CO_2-mediated vasodilative effects in vasculature not operating at reserve capacity (an effect similar to acetazolamide stress in prior PET studies [3]). Hyperoxia causes small, less specific BOLD increases due to elevations in the partial pressure of oxygen in veins as well as a small amount of binding of O_2 dissolved in plasma to venous deoxy-hemoglobin. Differences between these gas stimuli have been evaluated in detail [27], and qualitative

methods for accounting for arterial arrival times [28], partial volume effects [28], and differential endovascular signal have suggested that when appropriate post-processing procedures are implemented, hypercapnic hyperoxic stimuli correlate with CBF reactivity, as well as disease severity in moyamoya disease and atherosclerotic stenosis [16].

Limitations

First, SPECT or PET data were not acquired. Rather, we utilized ASL MRI perfusion imaging which has been directly compared with both SPECT and PET in the literature (for a review see [29] and references therein) and has been found to provide similar CBF values. This study sought to assess the feasibility of improving CCD diagnosis through non-invasive methods, and findings indicating a significant correlation between CCD (defined by asymmetric cerebellar CBF) with AICVR and AIWD provide the impetus to correlate non-invasive ASL-CBF weighted and BOLD-CVR weighted MR with PET or SPECT in future studies. Second, our study did not control for infarct volume; it is unclear that infarct volume is an independent determinant of CCD over infarct location [30]. Infarct location in the corticospinal tract has been shown to correlate better with Wallerian degeneration than infarct volume, thus corticospinal tract involvement was considered instead of stroke volume in this study [17]. Finally, CBF asymmetry values used to define CCD were based upon a region of interest covering a large portion of the cerebellum, and did not reflect measurements specific to known functional regions of the cerebellum such as the medial, intermediate, and lateral zones. Such stratification has previously revealed that the spatial distribution of supratentorial cortical lesions may affect metabolism in specific cerebellar regions, suggesting that hemodynamic function averaged across the entire cerebellum may dilute more pronounced region-specific changes [23].

Conclusion

Significant correlation between asymmetric cerebellar CVR and Wallerian degeneration in CCD subjects was observed utilizing non-invasive ASL and hypercapnic BOLD MRI, suggesting BOLD MRI may provide a noninvasive surrogate marker for CCD to study structural correlates and clinical consequences of CCD following supratentorial stroke.

References

1. Yamauchi H, Fukuyama H, Kimura J. Hemodynamic and metabolic changes in crossed cerebellar hypoperfusion. Stroke. 1992; 23:855–860. [PubMed: 1595105]
2. Yamauchi H, Fukuyama H, Nagahama Y, Nishizawa S, Konishi J. Uncoupling of oxygen and glucose metabolism in persistent crossed cerebellar diaschisis. Stroke. 1999; 30:1424–1428. [PubMed: 10390317]
3. Ito H, Kanno I, Shimosegawa E, Tamura H, Okane K, Hatazawa J. Hemodynamic changes during neural deactivation in human brain: a positron emission tomography study of crossed cerebellar diaschisis. Ann Nucl Med. 2002; 16:249–254. [PubMed: 12126094]
4. Kim SE, Choi CW, Yoon BW, et al. Crossed-cerebellar diaschisis in cerebral infarction: technetium-99m-HMPAO SPECT and MRI. J Nucl Med. 1997; 38:14–19. [PubMed: 8998142]
5. Lin DD, Kleinman JT, Wityk RJ, et al. Crossed cerebellar diaschisis in acute stroke detected by dynamic susceptibility contrast MR perfusion imaging. AJNR Am J Neuroradiol. 2009; 30:710–715. [PubMed: 19193758]

6. Machado A, Baker KB. Upside down crossed cerebellar diaschisis: proposing chronic stimulation of the dentatothalamocortical pathway for post-stroke motor recovery. Front Integr Neurosci. 2012; 6:20. [PubMed: 22661933]
7. Yamada H, Koshimoto Y, Sadato N, et al. Crossed cerebellar diaschisis: assessment with dynamic susceptibility contrast MR imaging. Radiology. 1999; 210:558–562. [PubMed: 10207444]
8. Liu X, Tian W, Qiu X, et al. Correlation analysis of quantitative diffusion parameters in ipsilateral cerebral peduncle during Wallerian degeneration with motor function outcome after cerebral ischemic stroke. J Neuroimaging. 2012; 22:255–260. [PubMed: 21699612]
9. Madai VI, Altaner A, Stengl KL, et al. Crossed cerebellar diaschisis after stroke: can perfusion-weighted MRI show functional inactivation? J Cereb Blood Flow Metab. 2011; 31:1493–1500. [PubMed: 21386854]
10. Kim SE, Lee MC. Cerebellar vasoreactivity in stroke patients with crossed cerebellar diaschisis assessed by acetazolamide and 99mTc-HMPAO SPECT. J Nucl Med. 2000; 41:416–420. [PubMed: 10716312]
11. Yamauchi H, Okazawa H, Sugimoto K, Kishibe Y, Takahashi M. The effect of deafferentation on cerebral blood flow response to acetazolamide. AJNR Am J Neuroradiol. 2004; 25:92–96. [PubMed: 14729536]
12. O'Gorman RL, Siddiqui A, Alsop DC, Jarosz JM. Perfusion MRI demonstrates crossed-cerebellar diaschisis in sickle cell disease. Pediatr Neurol. 2010; 42:437–440. [PubMed: 20472198]
13. Dani KA, Santosh C, Brennan D, Hadley DM, Muir KW. Crossed cerebellar diaschisis: insights into oxygen challenge MRI. J Cereb Blood Flow Metab. 2012; 32:2114–2117. [PubMed: 23047271]
14. Lu H, Donahue MJ, van Zijl PC. Detrimental effects of BOLD signal in arterial spin labeling fMRI at high field strength. Magn Reson Med. 2006; 56:546–552. [PubMed: 16894581]
15. Alsop DC, Detre JA, Golay X, et al. Recommended implementation of arterial spin-labeled perfusion MRI for clinical applications: A consensus of the ISMRM perfusion study group and the European consortium for ASL in dementia. Magn Reson Med. 201410.1002/mrm.25197
16. Donahue MJ, Dethrage LM, Faraco CC, et al. Routine clinical evaluation of cerebrovascular reserve capacity using carbogen in patients with intracranial stenosis. Stroke. 2014; 45:2335–2341. [PubMed: 24938845]
17. Mark VW, Taub E, Perkins C, Gauthier LV, Uswatte G, Ogorek J. Poststroke cerebral peduncular atrophy correlates with a measure of corticospinal tract injury in the cerebral hemisphere. AJNR Am J Neuroradiol. 2008; 29:354–358. [PubMed: 18024577]
18. Banks JL, Marotta CA. Outcomes validity and reliability of the modified Rankin scale: implications for stroke clinical trials: a literature review and synthesis. Stroke. 2007; 38:1091–1096. [PubMed: 17272767]
19. Jones KC, Hawkins C, Armstrong D, et al. Association between radiographic Wallerian degeneration and neuropathological changes post childhood stroke. Dev Med Child Neurol. 2013; 55:173–177. [PubMed: 23171053]
20. DeVetten G, Coutts SB, Hill MD, et al. Acute corticospinal tract Wallerian degeneration is associated with stroke outcome. Stroke. 2010; 41:751–756. [PubMed: 20203322]
21. Kim J, Lee SK, Lee JD, Kim YW, Kim DI. Decreased fractional anisotropy of middle cerebellar peduncle in crossed cerebellar diaschisis: diffusion-tensor imaging-positron-emission tomography correlation study. AJNR Am J Neuroradiol. 2005; 26:2224–2228. [PubMed: 16219826]
22. Forster A, Kerl HU, Goerlitz J, Wenz H, Groden C. Crossed cerebellar diaschisis in acute isolated thalamic infarction detected by dynamic susceptibility contrast perfusion MRI. PLoS One. 2014; 9:e88044. [PubMed: 24505372]
23. Liu Y, Karonen JO, Nuutinen J, Vanninen E, Kuikka JT, Vanninen RL. Crossed cerebellar diaschisis in acute ischemic stroke: a study with serial SPECT and MRI. J Cereb Blood Flow Metab. 2007; 27:1724–1732. [PubMed: 17311077]
24. Komaba Y, Mishina M, Utsumi K, Katayama Y, Kobayashi S, Mori O. Crossed cerebellar diaschisis in patients with cortical infarction: logistic regression analysis to control for confounding effects. Stroke. 2004; 35:472–476. [PubMed: 14739422]

25. Biersack HJ, Hartmann A, Friedrich G, et al. [Cause of crossed cerebellar diaschisis in cerebrovascular disease]. Nuklearmedizin. 1984; 23:227–230. [PubMed: 6335245]

26. Pantano P, Baron JC, Samson Y, Bousser MG, Derouesne C, Comar D. Crossed cerebellar diaschisis. Further studies. Brain. 1986; 109(Pt 4):677–694. [PubMed: 3488093]

27. Arteaga, DF.; Donahue, MJ.; Faraco, CC., et al. Vessel Wall Imaging in Young, Healthy Adults and Moyamoya Patients. Annual meeting of the International Society for Magnetic Resonance in Medicine; Toronto, Canada: 2015.

28. Faraco, CC.; Dethrage, LM.; Neill, M., et al. Cerebrovascular Reactivity Quantification in Patients with Intracranial Stenosis Before and After Surgical Revascularization. 22nd International Society for Magnetic Resonance in Medicine Scientific Meeting & Exhibition; Milan, Italy. 2014.

29. Donahue MJ, Strother MK, Hendrikse J. Novel MRI approaches for assessing cerebral hemodynamics in ischemic cerebrovascular disease. Stroke. 2012; 43:903–915. [PubMed: 22343644]

30. Sobesky J, Thiel A, Ghaemi M, et al. Crossed cerebellar diaschisis in acute human stroke: a PET study of serial changes and response to supratentorial reperfusion. J Cereb Blood Flow Metab. 2005; 25:1685–1691. [PubMed: 15931159]

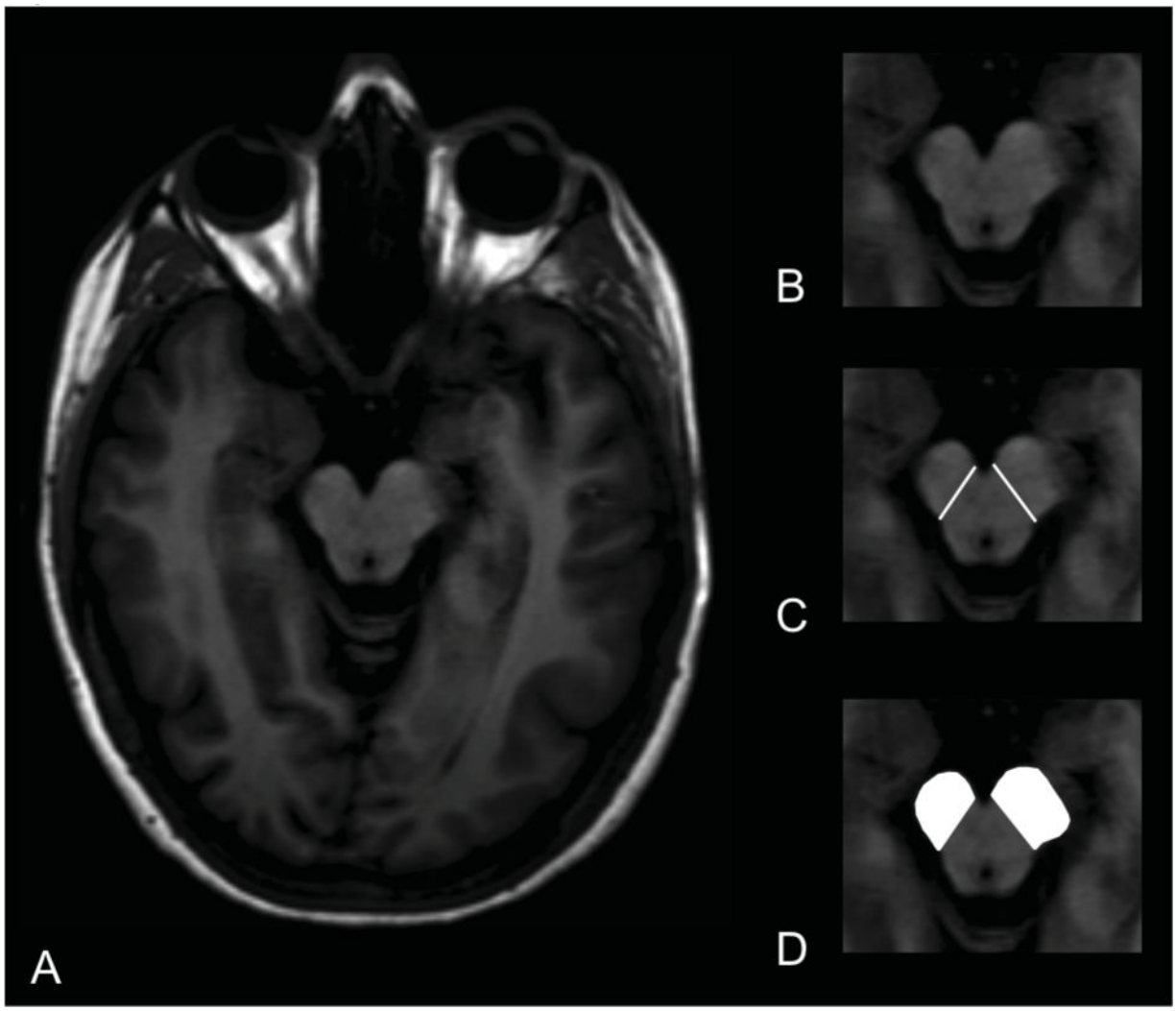

Figure 1.

Cerebral peduncle asymmetry index. T_1-weighted axial MRI image at level of maximum cerebral peduncle area (A). Magnified view of cerebral peduncles at same level (B). Medial border of cerebral peduncles delineated (C). Regions of interest drawn over cerebral peduncles (white, D). In this subject with a right hemisphere CST infarct (Pt ID 56), the right cerebral peduncle demonstrates Wallerian degeneration.

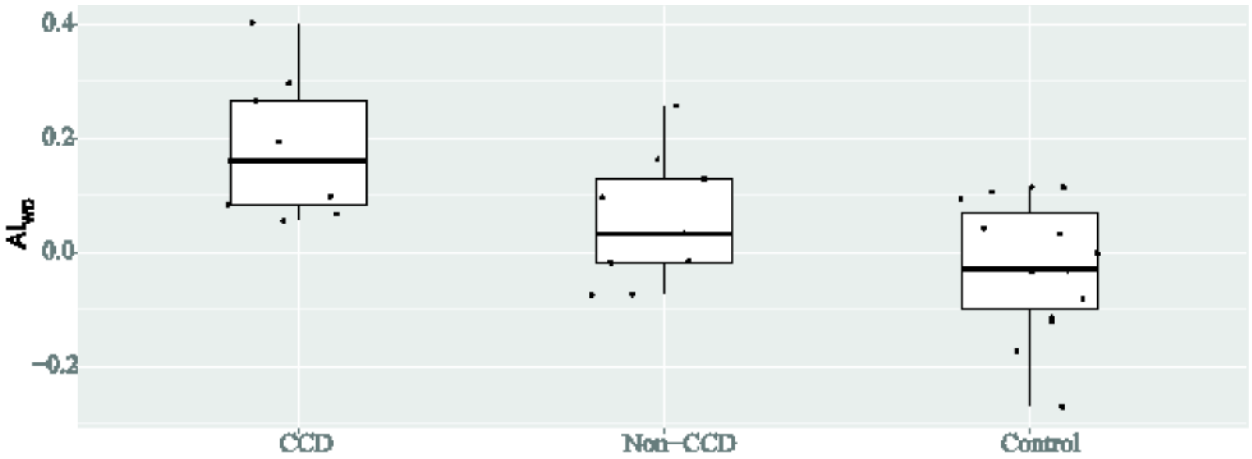

Figure 2.

Trend analysis for all subjects demonstrates a statistically significant ($p = 0.0004$) trend for Wallerian degeneration between subgroups, with Wallerian degeneration most frequent in subjects with CCD.

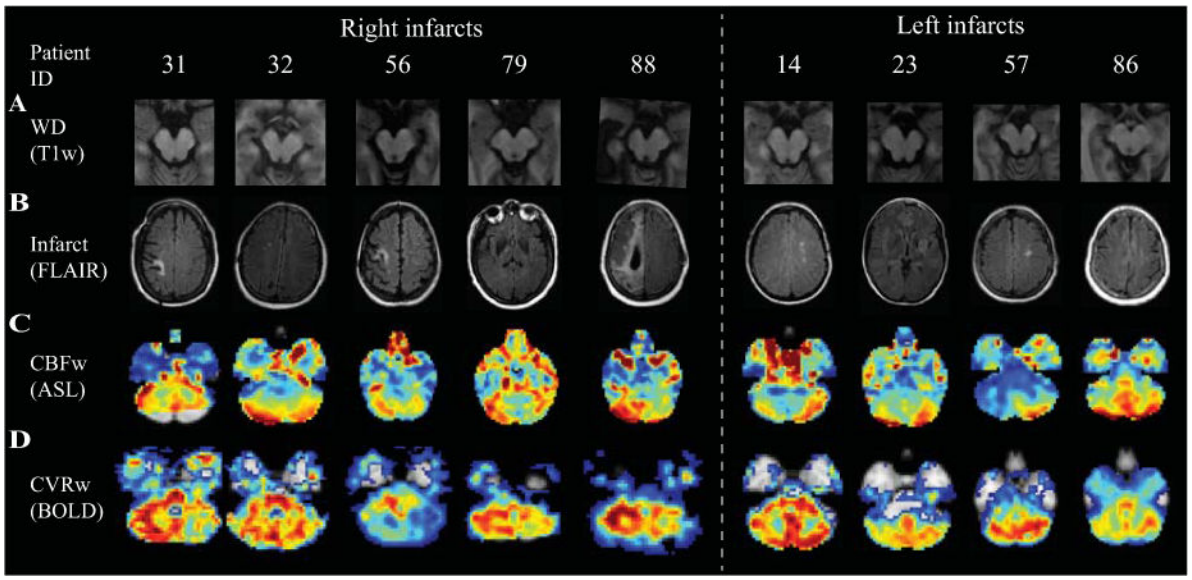

Figure 3.

T_1-weighted axial MRI at level of cerebral peduncles (A), representative FLAIR images at level of supratentorial infarct (B), CBF-weighted ASL (C), and BOLD CVR z-statistics (D) at level of cerebellar hemispheres for CCD subjects. In CCD subjects, cerebellar hemisphere CBF and CVR are decreased contralateral to supratentorial infarct. Wallerian degeneration causes volume loss in the cerebral peduncle ipsilateral to supratentorial infarct.

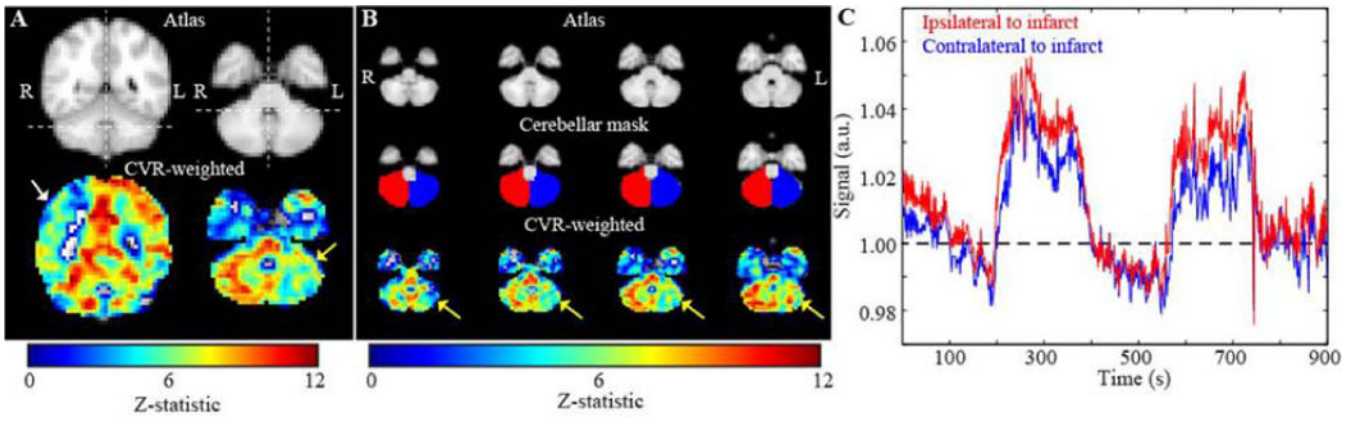

Figure 4.

Axial BOLD z-statistics reactivity and magnitude images with cerebellar ROI and signal intensity curve. This subject (Pt ID 31) had the most significant AI_{CVR}, due to CCD from a right CST infarct. The left (impaired) cerebellar hemisphere signal intensity curve (blue) is reduced, but not delayed, compared to the right (unimpaired) cerebellar hemisphere signal intensity curve (red).

Table 1

Inclusion and exclusion criteria. CCD=crossed cerebellar diaschisis. CBF asymmetry was defined as the relative CBF difference between cerebellar hemispheres using the cerebellar atlas (see Materials and Methods).

	Inclusion	**Exclusion**
Controls	1. Significant (>50%) intracranial stenosis	1. Any infarct on FLAIR MRI 2. Significant (≥ 50%) vertebrobasilar arterial stenosis
Non-CCD Infarct	1. Significant (>50%) intracranial stenosis 2. Supratentorial infarct on FLAIR	1. Significant (≥ 50%) vertebrobasilar arterial stenosis 2. Bilateral cerebral infarcts on FLAIR MRI 3. Acute or subacute infarct (<2 months)
CCD Infarct	1. Significant (>50%) intracranial stenosis 2. Supratentorial infarct on FLAIR 3. CBF asymmetry index outside 95% confidence interval of controls	1. Significant (≥ 50%) vertebrobasilar arterial stenosis 2. Bilateral cerebral infarcts on FLAIR MRI 3. Acute or subacute infarct (<2 months) 4. Posterior fossa infarct 5. Non-stroke etiology for Wallerian degeneration

Table 2

Asymmetry indices (AI) from control subjects (n=16) without infarcts.

Controls	Mean	Standard deviation	95% Confidence Interval
AI_{CBF}	0.003	0.095	[−0.045, 0.051]
AI_{CVR}	−0.007	0.076	[−0.046, 0.031]
AI_{WD} (reader 1)	−0.030	0.145	[−0.130, 0.043]
AI_{WD} (reader 2)	−0.017	0.108	[−0.072, 0.037]
AI_{WD} (mean)	−0.024	0.114	[−0.081, 0.034]

Table 3

Values obtained in subjects with infarcts. Crossed cerebellar diaschisis (CCD) subjects summarized above, whereas non-CCD subjects are summarized below. CST=corticospinal tract involvement (Y/N).

Group	ID	Age (yrs)	Sex	Motor	CST	AI.WD	AI.CBF	AI.CVR
CCD	88	58	F	3	Y	0.265	−0.177	−0.109
CCD	79	82	F	2	Y	0.055	−0.152	−0.063
CCD	56	43	M	3	Y	0.194	−0.109	−0.105
CCD	32	45	M	1	N	0.068	−0.051	−0.052
CCD	23	47	M	3	Y	0.082	−0.115	−0.066
CCD	14	34	F	2	N	0.402	−0.319	−0.058
CCD	31	25	F	2	Y	0.16	−0.131	−0.239
CCD	57	45	F	1	N	0.298	−0.118	−0.045
CCD	86	75	F	3	N	0.098	−0.074	0.047
Non-CCD	05	53	F	2	N	0.13	0.073	−0.025
Non-CCD	12	28	F	1	N	0.096	0.052	−0.005
Non-CCD	49	50	F	1	N	0.033	0.044	0.061
Non-CCD	54	33	F	1	N	0.163	0.136	0.01
Non-CCD	63	51	M	2	Y	−0.073	0.04	0.018
Non-CCD	73	47	F	3	Y	0.257	−0.016	0.004
Non-CCD	89	51	M	1	Y	−0.018	−0.024	0.067
Non-CCD	92	25	M	1	Y	−0.016	0.121	0.086
Non-CCD	16	69	M	1	Y	−0.075	0.079	0.015

Table 4

Mean CCD and nonCCD values for all subjects with infarcts.

Subjects with infarcts	Age (yrs)	Motor	AI.WD	AI.CBF	AI.CVR
CCD subjects	50.44	2.22	0.18[b]	−0.14	−0.08[a]
Non-CCD subjects	45.22	1.44	0.06	0.06	0.03

[a] = statistically significant by Wilcoxon Rank Sum test ($p < 0.01$),

[b] = statistically significant by trend analysis (CCD versus nonCCD versus controls) using Jonckheere-Terpstra test ($p < 0.001$). Higher motor score represents increased motor impairment.